Available online at www.sciencedirect.com

ScienceDirect

Ceramics International 40 (2014) 7185–7193

CERAMICS INTERNATIONAL

www.elsevier.com/locate/ceramint

# Mechanosynthesis of the multiferroic cubic spinel $Co_2MnO_4$: Influence of the calcination temperature

Maria Elenice dos Santos[a,d,*], Alicia Castro[b], Inmaculada Martinez[b], Paulo Noronha Lisboa-Filho[c], Octavio Peña[d]

[a]Grupo de Materiais Avançados, UNESP—Universidade Estadual Paulista, 17033-360 Bauru, SP, Brazil
[b]Instituto de Ciencia de Materiales de Madrid—ICMM—CSIC, 28049 Madrid, Spain
[c]Departamento de Física, Faculdade de Ciências,Universidade Estadual Paulista, 17033-360 Bauru, SP, Brazil
[d]Institut des Sciences Chimiques de Rennes, UMR 6226, Université de Rennes 1, 35042 Rennes, France

Received 27 November 2013; received in revised form 10 December 2013; accepted 12 December 2013
Available online 25 December 2013

**Abstract**

Multiferroic materials showing magnetoelectric coupling are required in various technological applications. Many synthetical approaches can be used to improve the magnetic and/or electrical properties, in particular when the materials exhibit cationic valence fluctuations, as in the $Co_2MnO_4$ cubic spinel. In this compound, Co and Mn ions are in competition at the tetrahedral and octahedral positions, depending on their various oxidation states. The $Co_2MnO_4$ was prepared following two techniques: by a soft chemical route based on a modified polymer precursor method, and by a mechanoactivation route. Both approaches yield polycrystalline powders, but their crystallites sizes and particles morphologies differ as a function of the calcination conditions. The magnetic characterization (ZFC/FC cycles, ordering temperatures, ferromagnetic coercive fields and saturation magnetizations) showed that the synthesis procedure influenced the physical properties of $Co_2MnO_4$ mainly through the size of the magnetic domains, which play an important role on the magnetic interactions between the Co/Mn cations.


*Keywords:* C. Magnetic properties; Multiferroic materials; Mechanoactivation; Thermal treatment; Microstructure

## 1. Introduction

Materials which are simultaneously ferroelectric and ferromagnetic (the so-called "multiferroic" materials) are of evident interest, being employed in various areas and deserving much attention nowadays because of their exciting physical properties [1–3]. A specific family among these materials concerns the spinels $AB_2O_4$, for which the crystal structure presents an arrangement between A cations located at tetrahedral positions, B cations placed at octahedral positions and oxygen anions [4,5]. Spinels are generally classified as normal or inverted but, according to the $(A_{1-i}B_i)[A_iB_{2-i}]O_4$ formulation, where $i$ is the inversion degree, random compositions with $0 < i < 1$ are easily formed [6]. The $Co_2MnO_4$ compound is a fully inverted cubic spinel containing Wyckoff positions, with cobalt and manganese cations located at 8a positions, tetrahedrically coordinated with the oxygen, and at 16d positions, octahedrically coordinated with oxygen, whereas oxygen is located at the 32e positions [7]. An interesting feature is the existence of metal valence fluctuations since the Co and Mn atoms can move between the tetrahedral and octahedral sites, exhibiting several oxidation states coexisting in the material [8] while a Jahn–Teller effect causes the distortion of the oxygen octahedra due to the $Mn^{3+}$–$Mn^{4+}$ exchange interactions [9–11].

The $Co_2MnO_4$ compound belongs to the $Co_{3-x}Mn_xO_4$ system, for which, at one end, the $Co_3O_4$ compound has a normal spinel structure with *Fd*-3*m* space group [12] whereas, at the other extreme, the $Mn_3O_4$ compound is a tetragonal haussmanite with $I4_1/amd$ space group [13]). Within this system, the $Co_2MnO_4$

*Corresponding author at: Grupo de Materiais Avançados, UNESP—Universidade Estadual Paulista, 17033-360 Bauru, SP, Brazil. Tel./fax: +55 1431 036 090.
*E-mail addresses:* e.santos@fc.unesp.br, elenice.dos-santos@univ-rennes1.fr (M.E.d. Santos).

0272-8842/$ - see front matter 
http://dx.doi.org/10.1016/j.ceramint.2013.12.057

compound ($x=1$) presents admirable physical and chemical properties (electric, magnetic and electrochemical [14,15]), in particular due to the $Co^{2+}/Co^{3+}$ and $Mn^{2+}/Mn^{3+}/Mn^{4+}$ presence. Bordeneuve et al. [15], using charge balance arguments applied to the $Co_{3-x}Mn_xO_4$ system, showed that many valence states are possible when Mn enters in the spinel structure to occupy the Co positions. Ríos et al. [8] studied the whole solid solution, from $x=0$ up to $x=3$, showing many possible valence combinations for Co and Mn, making clear that the $Co^{2+}$ and $Mn^{2+}$ ions (when present) should occupy the A sites whereas the $Co^{3+}$, $Mn^{3+}$ and $Mn^{4+}$ ions should occupy the B sites. Ahuja et al. [16] reinforced this idea in the case of the $Co_2MnO_4$ compound: $Co^{3+}$ ions occupy the octahedral B sites (16d) exhibiting a low spin state with no magnetic moment. It is found that, in the case of spinel systems, especially those containing Mn cations, the physical properties, in particular magnetic, are strongly dependent on the synthesis process and are related to a cation-deficiency due to variations in the oxidation state and/or due to oxygen-rich compositions [17]. Thus, the positions occupied by Co and Mn elements in this spinel structure, as well as the oxygen content, are highly dependent of the synthesis procedure.

Different synthesis approaches and thermal treatments can directly influence the appearance and/or combination of the $Co^{2+}/Co^{3+}$ and $Mn^{2+}/Mn^{3+}/Mn^{4+}$ valence states in $Co_2MnO_4$ [16,18,19], as well as the creation of oxygen vacancies [20]. On the other hand, from the point of view of nanomaterials, synthesis procedures employing high temperatures are inappropriate to obtain samples with high specific surface areas, because sintering favors the formation of large crystals.

We report herein the synthesis of $Co_2MnO_4$ by means of two different approaches: a modified polymeric precursors method (MPPM) [21,22] and a mechanochemical method (MS) [23,24]. During these two processes, the thermal treatment will be a critical point to compare the magnetic response of all samples. The MPPM approach allows controlling many parameters of the synthesis process, such as purity of reagents, temperature, time of reaction, pH, etc. These factors directly influence the magnetic behavior of the samples; as an example, a thorough study performed by our research group on the pH dependence, showed a net increase of the saturation magnetization ($M_S$) when the pH was modified from 1–7 [25]. Considering the spinel arrangement and since the MPPM, a soft chemical route, results in a polymeric resin in which the ions are dispersed inside the matrix [22,26], presence of metallic ions with quite different ionic radii may constitute a problem to obtain the expected stoichiometry of the desired materials [27]. In the case of the $Co_2MnO_4$ compound, this problem is not encountered since the ionic radii of Co (0.65 Å) and Mn (0.78 Å) are very similar; however, the calcination temperatures needed to obtain single phase samples using the MPPM approach, may be quite high. In contrast, the mechanochemical MS approach has excellent advantages when compared to MPPM since a pre-synthesis is achieved during the mechanoactivation stage and thus the expected stoichiometry can be obtained at much lower temperatures than those needed using the MPPM (or a classical ceramics) approach.

The magnetic nature of the $Co_2MnO_4$ compound is well known in the literature [7,17,19,28], reporting a ferrimagnetic character with an antiferromagnetic transition at around 180 K and a strong ferromagnetic behavior due to $Mn^{3+}$–$Mn^{4+}$ exchange interactions [11,29]. Joy and Date [7] and Borges et al. [19] reported a magnetic study of the $Co_2MnO_4$ material synthesized by different routes: first, by a standard ceramic method by mixing and heating the corresponding reagents and last, by the Pechini method. In all cases, the ferrimagnetic behavior is well kept; however, significant changes were observed regarding some specific magnetic parameters. Our goal is then, to make a thorough magnetic study and a full comparison between values which characterize this compound (transition temperature, Curie–Weiss temperature, effective moment, magnetization at $T=0$, coercive field, saturation magnetization, etc.), which can be slightly or drastically modified according to the different synthesis approaches.

## 2. Experimental section

Polycrystalline $Co_2MnO_4$ samples were synthesized by two differents approaches: by a modified polymeric precursors method (MPPM) [21,22] and by mechanochemical activation (MS) [23,24]. In the MPPM route, the reagents MnO (Aldrich > 99.9% purity) and $Co(NO_3)_2 \cdot 6H_2O$ (Aldrich > 99.9% purity) were weighed in stoichiometric amounts, to obtain 2 g of material. Firstly, the reagents were dissolved in water at 70°C; then, $HNO_3$ (15.2 mol/L, Aldrich > 99.9% purity) was added to MnO, followed by a chelating agent, a hydrocarboxylic acid ($C_6H_8O_7$, Aldrich > 99.9% purity), in 3:1=chelating: metal proportions. In order to form a polymeric resin, ethylene glycol ($C_2H_6O_2$, Aldrich > 99.9% purity) was then added in a chelating/alcohol mass ratio of 60/40. Finally, ethylenediamine ($C_2H_8N_2$, Aldrich > 99.9%) was added for a pH adjustement of 7. Pyrolisis was performed at 400 °C for 4 h, followed by successive annealings at 850 °C for 24 h and 1000 °C for 24 h, with intermediate grinding. In the MS route, $Co_2MnO_4$ was prepared from a stoichiometric mixture of MnO (Aldrich > 99.9% purity) and $Co_3O_4$ (Aldrich > 99.9% purity). Initially, the reagents oxydes were mixed using an agate mortar. About 10 g of mixed reagents were mechanically treated in a planetary mill (Fritsch Pulverisette 6) by using a tungsten carbide vessel with a volume of 250 $cm^3$ and seven tungsten carbide balls 2-cm in diameter and 63 g in weight each. The grinding vessel was rotated at 300 rpm for accumulating times (in total, up to 48 h), performing X-ray diffraction (XRD) analysis periodically to follow their evolution with milling. The mechanically treated powders were then calcined at various temperatures from 400 °C up to 1000 °C, for 2 h, systematically performing XRD at each step. The X-ray diffraction patterns were recorded at room temperature, in continuous mode, on a Bruker D8 Discover diffractometer with Cu-$K_{\alpha 1}$ radiation, $\lambda$=1.5406 Å, selected by a Ge(111) monochromator. The data were collected in the 5°-80° $2\theta$ range with a 0.02° step. Rietveld analysis was performed using the *Fullprof Suite* program [30,31], to minimize the difference between experimental and calculated XRD diagrams. The parameters adjusted in the least squares refinement

were: lattice parameters, atomic positions, atomic sites occupancies, atomic thermal vibrational parameters, isotropic and anisotropic, peak shape and asymmetry parameters, preferred orientation, background function, $2\theta$-zero correction and scale factor. A Thompson–Cox–Hasting pseudo-Voigt profile was used in order to resolve the instrumental, strain and size contributions to the peak broadening. In order to compare size grains and morphologies, the microstructures were examined by scanning electronic microscopy (SEM) using a JEOL JSM 6301F equipment, whereas the X-ray energy dispersion spectra (EDS) were collected on a JEOL JSM 6400-OXFORD detector. Magnetic measurements were carried out in a Quantum Design MPMS-XL5 SQUID (superconducting quantum interference device) magnetometer between 2 and 300 K. All samples were studied under identical conditions. Zero-field-cooled (*ZFC*)/field-cooled (*FC*) cycles were performed under low applied fields, typically 100 Oe; for this, the sample was first cooled down to the lowest temperature (2 K) in the absence of an external field and subsequently warmed up under the applied field while recording the data (ZFC mode). In a second step, the sample was cooled down under the same applied field (FC mode). Magnetization $M(H)$ loops were recorded at 10 K, as a function of field, with the field varying between −50 kOe and 50 kOe.

## 3. Results and discussion

### 3.1. Structural characterization of $Co_2MnO_4$

Fig. 1 shows the XRD patterns for $Co_2MnO_4$ samples synthesized by the MS method at 600 °C, 700 °C, 800 °C, 900 °C and 1000 °C and by the MPPM method at 1000 °C. A cubic spinel structure, *Fd*-3*m* (227) space group (JCPDS-ICDD Card no. 84-0482), was observed for all samples; Bragg peaks (111, 220, 311, 222, 400, 422, 333, 440, 620, 533 and 622) were indexed accordingly. No secondary phases were observed on any XRD pattern; in particular the MS_600 sample, expected to show some impurity phases due to a low calcination temperature, presented a monophasic XRD pattern, within the accuracy of the XRD technique.

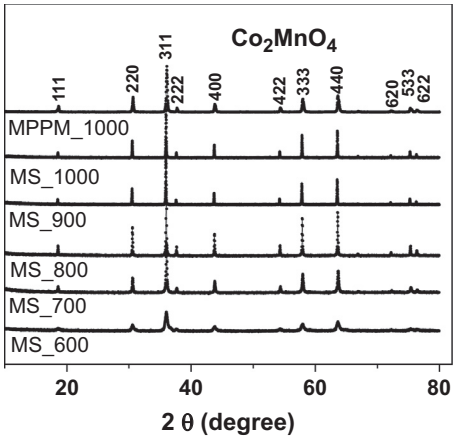


Fig. 1. X-ray diffraction patterns indexed in a cubic spinel *Fd*-3*m* (227) space group, for $Co_2MnO_4$ samples synthesized by the MS method for 2 h at given temperatures (MS_600, MS_700, MS_800, MS_900 and MS_1000), compared to a sample synthesized by the MPPM method at 1000 °C during 24 h (MPPM_1000 sample).

In order to confirm the purity of our materials, the XRD data for all samples (except for MS_600 which presented wide background and low intensity Bragg peaks) were refined by the Rietveld method using the *Fullprof Suite* program. Fig. 2 compares results for samples MS_800 and MPPM_1000. Fig. 2(a) shows the Rietveld refinement for the MS_800 sample, with a goodness of fit $\chi^2$ of 1.12 and no traces of any secondary phase. This fact proves the efficiency of the mechano-activated synthesis to obtain a single-phase $Co_2MnO_4$ material, a result which is only achieved at 1000 °C when synthesized by the MPPM method [29]. Fig. 2(b) shows the Rietveld refinement for the sample elaborated by the MPPM method and synthesized at 1000 °C (MPPM_1000). Analyzing these data and comparing them with the magnetic results (§0.3.3.), we can get a broad view and good understanding of the intrinsic behavior of the $Co_2MnO_4$ material, since no impurities were evidenced through the structural characterization (XRD and Rietveld refinement) nor through the magnetic measurements, except for the MS_600 sample as it will be discussed in Section 3.3. Indeed, although both spectra (Fig. 2(a) and (b))

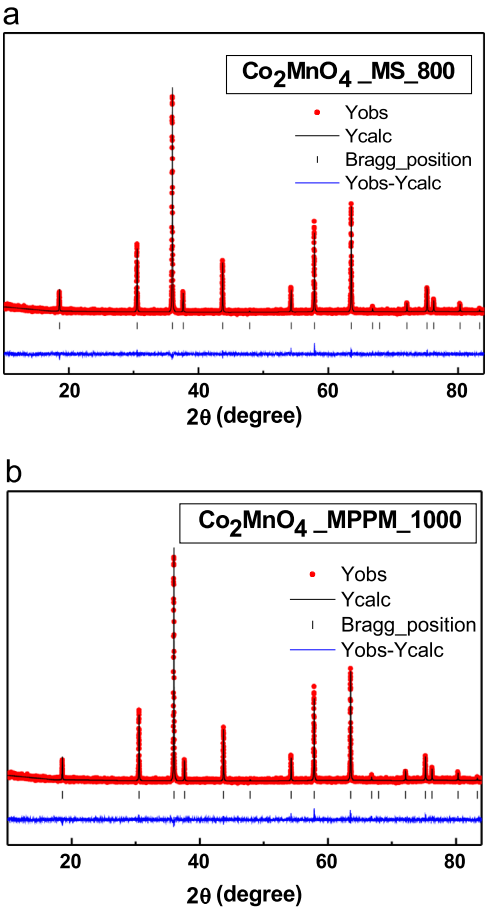


Fig. 2. Rietveld refinement of the powder XRD data of $Co_2MnO_4$ samples elaborated by: (a) the MS technique and calcined at 800 °C, and (b) the MPPM method and synthesized at 1000 °C. Observed and calculated intensities are represented by dots and solid lines, respectively, and vertical bars are the Bragg reflection position markers. The difference pattern between observed and calculated data is shown at the bottom.

look similar, the refined data, the cell parameters and the crystallites sizes strongly depend on the synthesis procedure and thermal treatment, as indicated in Table 1 and discussed here below.

### 3.2. Microstructural aspects

All samples concerned by this study, annealed at 600 °C, 700 °C, 800 °C, 900 °C and 1000 °C, showed a significant effect of peak broadening, indicating that the samples consisted of small crystallites, whose size and shape changed with temperature. The crystallites size was estimated from the most intense Bragg peak (311) of the XRD data, using the Scherrer equation [32]. A linear increase of the size was observed for materials synthesized by the MS route, starting at 600 °C and ending at 900 °C (Fig. 3). To be noticed that the MS_900 and MS_1000 samples show similar crystallite size, confirming that $Co_2MnO_4$ reached a stability limit with temperature when obtained by mechanoactivation. In contrast, when looking at the crystallites size of the sample synthesized by the mechanochemical activation method (MS_1000) compared to the sample elaborated by the polymer technique (MPPM_1000), although both materials were annealed at the same temperature (1000 °C), differences are striking, reinforcing the idea that the synthetical approach is an important parameter to be considered when obtaining materials with good magnetic performance. In fact, the size of the magnetic domains are directly correlated to the size of crystallites and, therefore, this will result in important changes in the intrinsic magnetic properties of the $Co_2MnO_4$ compound, as it will be discussed later (§0.3.3).

Although we cannot visualize any significant difference on the refined profile of both materials, since they exhibit the same Bragg peaks and the same crystallographic planes, analysis of the cell parameters indicates a strong dependence with the synthesis procedure (Table 1). Fig. 3 compares the cell parameters, as obtained after the Rietveld refinement, for all materials discussed above. A systematic increase of the lattice parameter can be observed for samples prepared by the mechanochemical technique, increasing from 8.253–8.317 Å when calcined from 600 °C–1000 °C. This last value is, however, much higher than the one obtained for samples prepared by the polymer method, of the order of 8.274 Å (Fig. 3 and Ref. [29]) or other techniques of synthesis [15,27,33]. Several hypotheses can be forwarded to explain such difference. Firstly, the oxygen content, which may depend on the synthesis procedure (atmosphere and annealing temperature). The work of Naka et al. [33] showed, however, almost no variation of the lattice parameter of $Co_{3-x}Mn_xO_4$ (for $x=2$) after oxygen or air annealings at 1000 °C. Also, the MS and MPPM samples under discussion were annealed under similar conditions of temperature and atmosphere environment. Particles size can be invoked since, by looking at Fig. 3, they seem to be strongly correlated with the evolution of the cell parameter. This is a quite plausible explanation, although it is hard to believe that, among all papers published in the literature concerning the $Co_2MnO_4$ spinel, no one has reported such high values for the cell parameters, independently if the material has been prepared from metal oxides [27], from carbonates and nitrates [33], from oxalic precursors [15] or from oxalates prepared from metal sulfates [17]. The most appropriate hypothesis to explain such difference in lattice parameters may be subtle variations in the cationic arrangement at the tetrahedral and octahedral positions. Bordeneuve et al. [15] have listed several possible cationic distributions proposed by different authors based on various experimental techniques (electrical conductivity, XRD, magnetic properties, neutron diffraction, etc.). The crystallographic arrangement of cationic species such as $Co^{2+}$, $Co^{3+}$, $Mn^{2+}$, $Mn^{3+}$ or $Mn^{4+}$, will have a direct

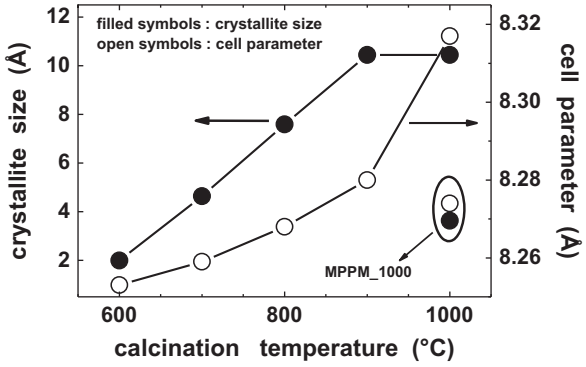


Fig. 3. Crystallite size (in Å, ±0.1) calculated from the 311 Bragg peak and cell parameter $a$ (in Å, ±0.007) for samples MS_600, MS_700, MS_800, MS_900 and MS_1000 as a function of the calcination temperature. Lower right-hand side: corresponding parameters for the MPPM_1000 sample.

Table 1
Crystallographic parameters obtained after Rietveld refinement of the XRD data for samples MS_600, MS_700, MS_800, MS_900, MS_1000 and MPPM_1000. The $R$ values correspond to: the weighted-profile ($R_{wp}$), the statistically expected residual ($R_{exp}$), the Bragg intensity $R$ value ($R_{Bragg}$). Also given: the goodness of fit ($\chi^2$), the cell parameter, the unit cell volume and the crystallite size calculated from the 311 Bragg peak using the Scherrer's equation.

| $Co_2MnO_4$ | $R_{wp}$ (%) | $R_{exp}$ (%) | $R_{Bragg}$ (%) | $\chi^2$ | $a$ (Å) (±0.007) | $V$ (Å$^3$) (±0.005) | Crystallite size (Å) (±0.1) |
|---|---|---|---|---|---|---|---|
| MS_600 | – | – | – | – | 8.253 | 562.190 | 1.99 |
| MS_700 | 11.30 | 6.90 | 9.88 | 1.63 | 8.259 | 563.339 | 4.64 |
| MS_800 | 12.29 | 10.97 | 11.40 | 1.12 | 8.268 | 565.203 | 7.59 |
| MS_900 | 14.20 | 10.52 | 10.65 | 1.35 | 8.280 | 567.664 | 10.44 |
| MS-1000 | 13.33 | 11.20 | 10.37 | 1.19 | 8.317 | 575.306 | 10.44 |
| MPPM_1000 | 14.13 | 10.24 | 11.06 | 1.38 | 8.274 | 566.430 | 3.63 |

incidence on the cell parameter because of their different ionic radii. However, our basic idea of a charge balance of the type $Co^{2+}\left[Co_x^{2+}Co_{1-x}^{III}Mn_{1-x}^{3+}Mn_x^{4+}\right]O_4$ ($Co^{III}$ in a low spin state) in our both sets of materials is hard to be confirmed by magnetic measurements [29]. Any redistribution of cations involving subtle valence changes will result into almost constant values of the effective moment ($\mu_{eff}\sim 8.2\ \mu_B$), knowing that magnetic species will compensate each other [$(\mu_{Co}^{2+})=(\mu_{Mn}^{4+})=3.87\ \mu_B$; $(\mu_{Co}^{3+})=(\mu_{Mn}^{3+})=4.90\ \mu_B$] [29].

Fig. 4 shows the SEM micrographs of the six $Co_2MnO_4$ samples discussed in this work. Samples prepared by mechanoactivation and calcined for 2 h at temperatures ranging from 600 °C up to 1000 °C are shown from Fig. 4(a)–(e). An evident evolution in their form and size is seen as a function of the calcination temperature, with homogeneous agglomeration of the particles and a steady increase in the particle′s size, as already inferred from the XRD data analysis. Furthermore, qualitative changes can be observed when passing from 800 °C to 900 °C and 1000 °C since particles progressively adopt a rounded shape and tend to reduce the number of grain boundaries.

For comparison, the MPPM_1000 sample synthesized at 1000 °C is shown in Fig. 4(f) under the same magnification factor ( × 10,000) as for all other images. Striking differences are observed between samples MS_1000 and MPPM_1000 thermally treated at the same temperature, although the MPPM_1000 sample (Fig. 4(f)) was synthesized for 24 h while the MS_1000 sample (Fig. 4(e)) was calcined for only 2 h. It can be immediately seen, for instance, that in the case

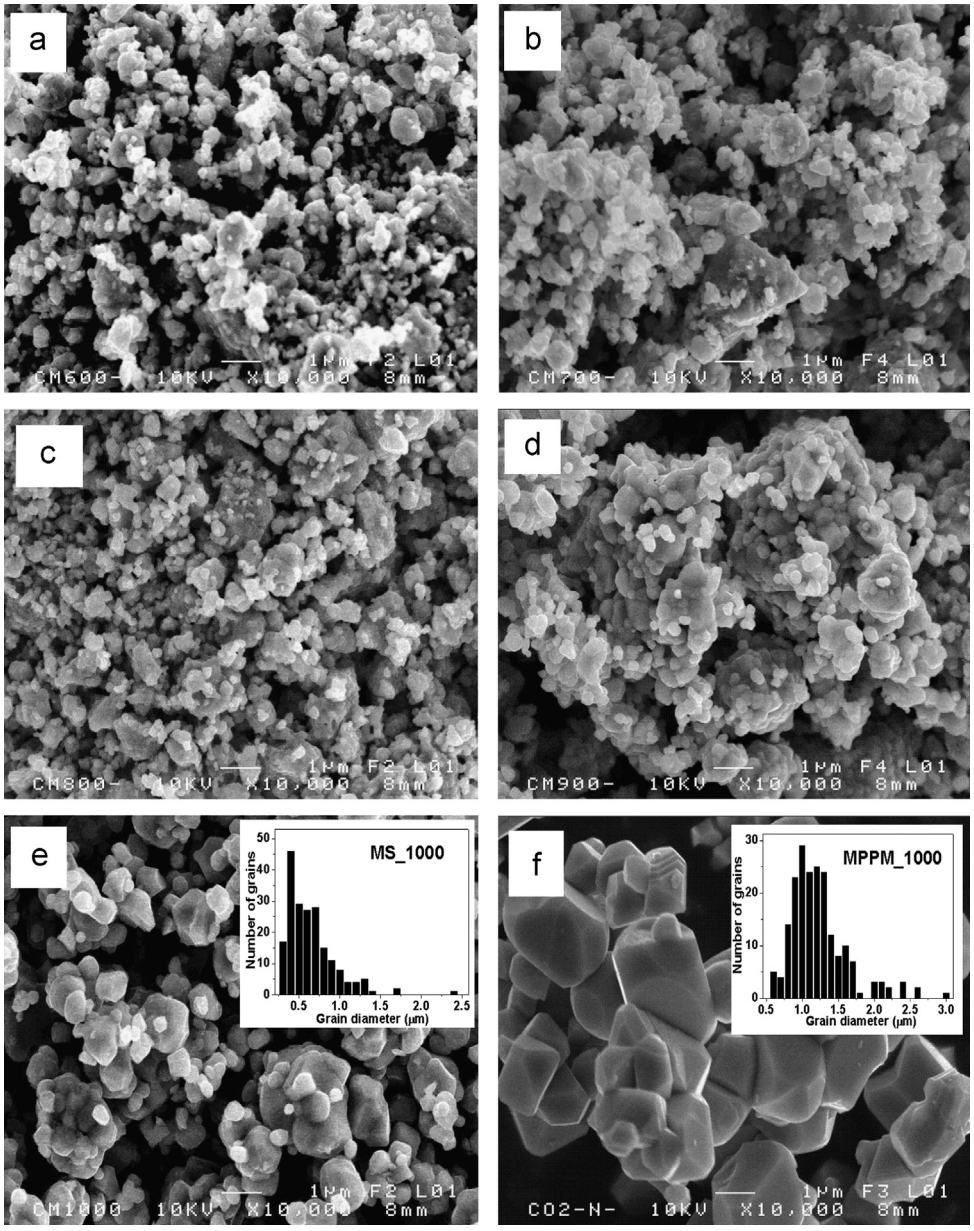


Fig. 4. Scanning electron microscopy (SEM) images for $Co_2MnO_4$ samples synthesized by the mechanochemical method (MS) and heat-treated at (a) 600 °C, (b) 700 °C, (c) 800 °C, (d) 900 °C and (e) 1000 °C for 2 h. (f) Sample synthesized by the modified polymer precursors method (MPPM) and heat-treated at 1000 °C for 24 h. Inserts in (e) and (f) indicate the particles size distribution, as calculated by using the *Image J* program.

of the MPPM_1000 sample, the grains have well defined crystal facets and adopt a cubic shape typical of the cubic spinel structure; in addition, grains are much larger, probably due to the duration of the calcination procedure, resulting in a reduced number of grain boundaries, which typically act as pinning centers in the ferromagnetic irreversible cycles [34].

A particular remark can be made at this point concerning the crystallites size (Fig. 3) compared to the particles size (inserts, Figs. 4(e) and (f)). Indeed, the crystallite size is evaluated from crystallographic data, involving the (311) Bragg peak analyzed by the Rietveld technique and the Scherrer′s equation. It does involve, then, nanosized information given by crystallographic reticular properties, and its evolution with the synthesis conditions is clearly demonstrated in Fig. 3. On the contrary, inserts in Fig. 4 show macroscopic details, as seen through agglomerates of micrometer dimensions forming blocks or particles; their morphological evolution as a function of calcination conditions are clearly seen in the inserts statistically calculated by using the *Image J* program (*Image Processing and Analysis in Java*).

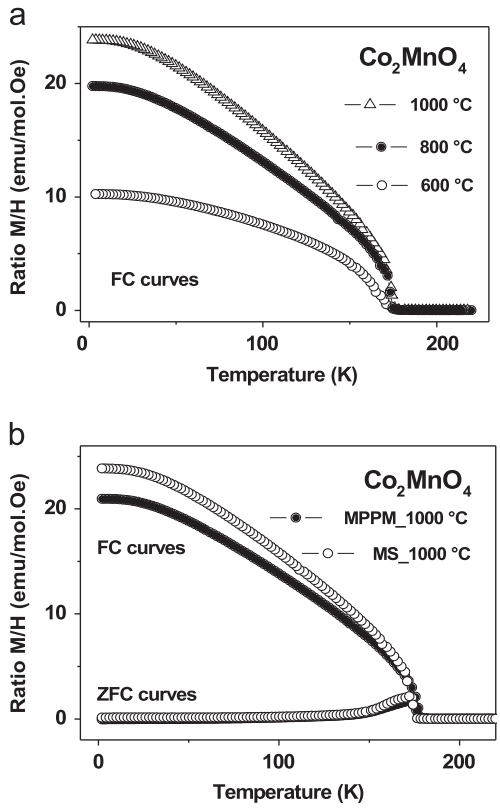


Fig. 5. (a) Temperature dependence of the field-cooled (*FC*) magnetization for $Co_2MnO_4$ synthesized by the MS method at given temperatures. (b) ZFC/FC magnetization cycles for $Co_2MnO_4$ synthesized by the MS and the MPPM methods at 1000 °C (all samples measured under an applied field $H_{app}$ of 100 Oe).

### 3.3. Magnetic properties of $Co_2MnO_4$

Temperature dependence of the field-cooled (*FC*) magnetization of samples synthesized by the MS method and thermally treated at 600 °C, 800 °C and 1000 °C, are shown in Fig. 5(a). A strong ferromagnetic behavior is immediately seen, mainly coming from the double-exchange interaction between $Mn^{3+}$ and $Mn^{4+}$ ions. For spinel compounds $AB_2O_4$, other magnetic interactions are expected between ions *A* and/or *B* due to specific intra-site and inter-site exchanges, which participate to the basic magnetic properties in the paramagnetic as well as in the ordered states. Among all these, the intra-site ferromagnetic exchange between Mn ions sitting at the octahedral position is the most important, whereas the $J_{AA}$ interactions at the tetrahedral sites between $Co^{2+}$–$Co^{2+}$ moments tend to cancel out since the cobalt spins point into opposite directions, as in the case of the $Co_3O_4$ spinel [13,35]. However, the Jahn–Teller effect associated to the $Mn^{3+}$ ion provokes a structural distortion and tends to deviate the antiparallel alignment of the $Co^{2+}$ spins adopting a canted-like state which enhances the ferromagnetic component. Thus, a competition between ferromagnetic (FM) and antiferromagnetic (AFM) interactions in $Co_2MnO_4$ leads to a ferrimagnetic behavior, as evidenced by the peak-like *ZFC* magnetization (Fig. 5(b)) and the strong negative Curie–Weiss temperature (ca. −630 K [29]).

Several features are worth noticing in Fig. 5(a). First of all, the magnetization values $M_{FC}(T=0)$, as defined by the extrapolation of the FC magnetization to $T=0$, change considerably as the calcination temperature is increased from 600 °C–1000 °C. Secondly, the critical temperature $T_C$ stays essentially invariant, although there is a slight but systematic increase from 171 K up to 176 K, for calcination temperatures from 700 °C up to 1000 °C. Other magnetic parameters are listed in Table 2, in particular $T_{max}$ corresponding to the temperature at which the *ZFC* magnetization attains a maximum (see Fig. 5(b)). For all these, we can remark that there is no much change between samples calcined at 900 °C or 1000 °C, meaning that we have

Table 2
Magnetic parameters for $Co_2MnO_4$ compounds synthesized by the MS and MPPM methods. $M_{FC}$, extrapolation of the FC curves to $T=0$; $T_C$, transition temperature; $T_{max}$, temperature value of the magnetization peak of the ZFC mode; $H_C$, coercive field; $M_S$, value of the magnetization at the highest working field (50 kOe).

| $Co_2MnO_4$ | $M_{FC}$ ($T=0$) (emu/mol) | $T_C$ (K) | $T_{max}$ (K) | $H_C$ (Oe) | $M_{50\,kOe}$ ($H=50$ kOe) ($\mu_B$) |
|---|---|---|---|---|---|
| MS_600 | 10.25 | 173 | 156 | 5300 | 0.51 |
| MS_700 | 12.26 | 171 | 162 | 8900 | 0.44 |
| MS_800 | 19.77 | 175 | 169 | 6300 | 0.59 |
| MS_900 | 23.91 | 176 | 172 | 4450 | 0.64 |
| MS_1000 | 23.90 | 176 | 172 | 3850 | 0.64 |
| MPPM_1000 | 21.00 | 178 | 172 | 3390 | 0.63 |

reached a limit for this compound. It is conceivable that at higher calcination temperatures, the volatility of Co and vacancies caused by oxygen departure directly influence the magnetic behavior of $Co_2MnO_4$ because of slight changes in stoichiometry. At this point we should remark the particular case of the sample calcined at 600 °C: values listed in Table 2 do not follow the same trend as those for samples calcined from 700 °C–1000 °C. This is in fact due to an incomplete reaction, as it will become quite obvious when we will discuss our results of the magnetization loops $M(H)$. For this reason, our discussion mainly involves samples calcined at 700 °C and above.

Knowing from the literature that the physical properties (in particular, magnetic) are greatly dependent on the grains size and since our main goal in this work is to compare samples obtained by two different synthesis routes, we show in Fig. 5(b) the zero-field-cooled (*ZFC*) and field-cooled (*FC*) magnetizations for $Co_2MnO_4$ prepared by the mechanochemical approach MS and by the modified polymer precursors method MPPM, and calcined under identical conditions of environment (air) and temperature (1000 °C). It is quite notorious that the synthesis method influences significantly the magnetic properties of this system, in particular the $M_{FC}$ value, which increases from 21.00–23.90 emu/mol whereas the transition temperature $T_C$ slightly decreases from 178 K to 176 K, for samples prepared by the MPPM and MS techniques, respectively (Table 2). However, the ferrimagnetic character of the $Co_2MnO_4$ compound is maintained in both samples, preserving their main magnetic features such as a paramagnetic state above $T_C$, a well-defined *AFM* transition with a narrow and asymmetric peak around the *ZFC* maximum of 172 K and an evident *FM* behavior, as seen in the *FC* curves.

To explain these differences, we must recall the different magnetic interactions at both tetrahedral and octahedral sites of the cubic spinel. The most important among such interactions are those occurring at the octahedral sites between the mixed-valence $Mn^{3+}$ and $Mn^{4+}$ ions, of ferromagnetic character. Then it is quite possible that the different synthesis procedures adopted in this work have a consequence on the relative amount of $Mn^{3+}$–$Mn^{4+}$ pairs through oxygen stoichiometry and/or sites occupation, as already discussed above concerning the cell parameters data. As a result, different $M_{FC}(T=0)$ saturation values are obtained from the *FM* magnetization curves, being optimal in the mechanoactivated procedure. On the other hand, the *ZFC* curves look quite similar in both cases, except for a slightly higher value of $T_C$ for the MPPM material. This invariance may be explained by intrasite $J_{AA}/J_{BB}$ and intersite $J_{AB}$ exchanges at the tetrahedral sites, which do not exhibit notable changes [29].

A further comparison between both techniques can be made regarding the magnetization cycles as a function of the applied field, that is, the $M(H)$ loops performed at 10 K with the magnetic field varying from −50 kOe up to +50 kOe. Prior to this, we should discuss the effect of the calcination temperature on samples prepared by the mechano-activated method. Fig. 6 shows the $M(H)$ loops for samples calcined at 600 °C, 800 °C and 1000 °C. The overall pattern is similar for all three samples: well-defined hysteresis loops with a "saturation" magnetization $M_{50\,kOe}$ (defined as the value attained under our maximum applied field of 50 kOe) and coercive fields $H_C$ (defined as the value of the magnetic field

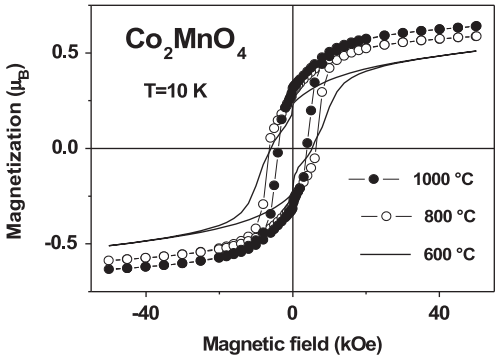


Fig. 6. Magnetization loops measured at $T=10$ K of the $Co_2MnO_4$ material synthesized by the MS method at given temperatures.

when the $M(H)$ curve reaches the zero-value at $M=0$). Both parameters, $M_{50\,kOe}$ and $H_C$, are strongly dependent on the calcination conditions, although having different origins. The "saturation" magnetization is directly related to the ferromagnetic exchange $Mn^{3+}$–$Mn^{4+}$, which is optimized during sintering and subsequent increase in size of grains and magnetic domains. On the contrary, the coercive field is directly related to the number of pinning centers. At weak sintering effect (i.e., low calcination temperature and small grains), the number of pinning centers is larger and therefore, the coercive fields are higher. Table 2 shows a factor of 2–2.5 between the $H_C$ values for samples calcined at 700 °C and 1000 °C, whereas $M_{50\,kOe}$ gradually increases towards a limiting state, since the values for 800 °C and 1000 °C are very close. For completeness, we should mention a third phenomenon seen in Fig. 6 for the sample calcined at 600 °C, of spurious origin since the clear anomaly in the $M(H)$ curve near $H=0$ is due to an incomplete reaction, as already discussed above.

Fig. 7 compares the magnetization loops recorded at low temperature, for samples elaborated by the MS technique (Fig. 7, left-hand panel) and by the MPPM method (Fig. 7, right-hand panel), calcined under similar conditions (in air and at 1000 °C). The overall behavior is substantially similar although the magnetic parameters differ (Table 2). The decrease of the coercive field (from $H_C=3850$ Oe to 3390 Oe, for samples synthesized by the MS and MPPM techniques, respectively), may be due to a longer calcination time (24 h for MPPM, 2 h for MS), which makes the particles grow larger as the sintering process takes longer. Larger ferromagnetic domains may also explain the more-regular rectangular-shaped ferromagnetic loop observed in the insert, Fig. 7, right-hand panel, for the MPPM sample, as compared to the MS sample calcined at 1000 °C. On the contrary, the saturation value of the magnetization ($M_{50\,kOe}$) decreases slightly (from 0.64 to 0.63 $\mu_B$) between both samples, implying that the ferromagnetic exchange is optimum for samples prepared by the mechanoactivation MS technique.

## 4. Conclusions

A comparative study of two synthesis procedures was presented in this work, one based on a wet chemical method using polymer precursors, the other by mechanoactivation milling of solid-state oxide reagents. The X-ray data and Rietveld refinements

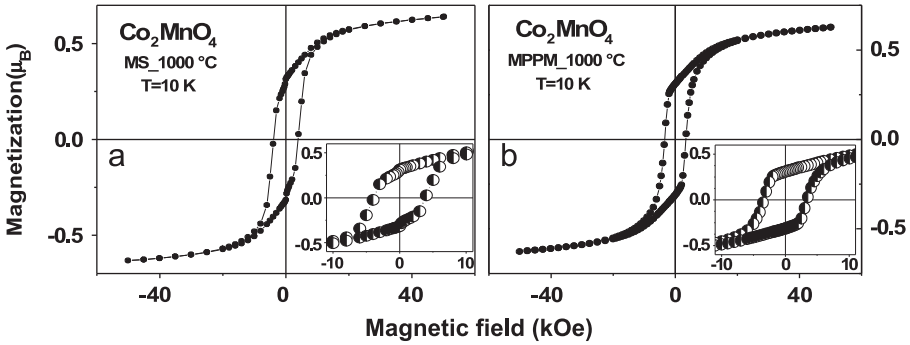


Fig. 7. Magnetization loops measured at $T=10$ K of the $Co_2MnO_4$ material synthesized by the MS (left) and the MPPM (right) methods at 1000 °C. The inserts zoom the irreversible part of the magnetization loop.

confirmed the inverse spinel structure of the $Co_2MnO_4$ compound, the absence of spurious phases and the good crystallinity for all samples, with $Co^{2+}$ occupying the tetrahedral positions and $Co^{3+}$, $Mn^{3+}$ and $Mn^{4+}$ in competition to occupy the octahedral sites.

Analyzing the data (XRD, SEM and magnetic measurements) for samples synthesized by the mechanochemical MS technique and annealed from 600 °C up to 1000 °C, we found that pure phases were obtained at calcination temperatures as low as 800 °C, while both the morphology and shape of the sample radically changed as a function of temperature and synthetical technique. After a linear increase with the calcination temperature, the size of the crystallites reached constant values at 900 °C, indicating a stability limit for samples presynthesized by a mechanoactivation technique. On the contrary, the material prepared by the polymeric precursor method MPPM showed large agglomerates due to a prolonged thermal treatment at high temperatures while exhibiting small crystallites size and lower cell parameters.

Other parameters like the ferromagnetic coercive field $H_C$ or the magnetic transition temperature $T_C$ also reached constant values, confirming that an optimum situation is attained both in the magnetic properties and in the microstructural aspects of these materials when elaborated by mechanoactivation. Of particular interest is the fact that the coercive field $H_C$ correlated well with the size of the magnetic domains, reaching its lowest value ($\sim$3850 Oe) at the highest calcination temperature when the crystallites attain their largest dimension and when the density of grains boundaries decreased.

Through this report we have shown that the mechanoactivation method MS had a clear advantage over the MPPM method thanks to the fact that optima magnetic and crystallographic parameters are attained at rather low calcination temperatures, of the order of 800 °C, several hundreds of degrees centigrade below the sintering conditions necessary in other more classical synthetical procedures. From this comparative work, we may conclude: first, that magnetic measurements, complemented by the Rietveld refinement, are powerful tools to detect spurious magnetic phases and, second, that adequate synthesis routes employing much lower sinterization temperatures are the most convenient way to study the intrinsic physical properties, in this case the magnetic behavior of the spinel oxide $Co_2MnO_4$.

## Acknowledgments

Authors are thankful to FAPESP Grant 2007/08072-0 and Spain′s project MAT2001-23709. The authors also acknowledge the bilateral exchange programs France–Brazil CAPES-COFECUB, Project no.706/11. M.E. Santos in a Joint Ph.D International Program, UNESP—Université de Rennes.

## References

[1] N.A. Spaldin, S-W. Cheong, R. Ramesh, Multiferroics: past, present and future, Phys. Today 63 (2010) 38–43.
[2] D. Khomskii, Classifying multiferroics: mechanisms and effects, Physics 20 (2009) 2–6.
[3] E. Dagotto, J. Burgy, A. Moreo, Nanoscale phase separation in colossal magnetoresistance materials: lessons for the cuprates?, Solid State Commun 126 (2003) 9–22.
[4] P.N. Lisboa-Filho, C. Vila, M.S. Góes, C. Morilla-Santos, L. Gama, E. Longo, W.H. Schreiner, C.O. Paiva-Santos, Composition and electronic structure of $Zn_{7-x}M_xSb_2O_{12}$ (M=Ni and Co) spinels compound, Mater. Chem. Phys. 85 (2004) 377–382.
[5] Y.H. Hou, Y.J. Zhao, Z.W. Liu, H.Y. Yu, X.C. Zhong, W.Q Qiu, D.C. Zeng, L.S. Wen, Structural, electronic and magnetic properties of partially inverse spinel $CoFe_2O_4$: a first principles study, J. Phys. D: Appl. Phys. 43 (2010) 445003–445007.
[6] C.B. Azzoni, M.C. Mozzati, L. Malavasi, P. Ghigna, G. Flor, Magnetic and X-ray diffraction investigation on $Mg_{1-x}Mn_{2+x}O_4$ spinels,, Sol. State Commun. 119 (2001) 591–595.
[7] P.A. Joy, S.K. Date, Unusual magnetic hysteresis behavior of oxide spinel $MnCo_2O_4$, J. Magn. Magn. Mater. 210 (2000) 31–34.
[8] E. Ríos, P. Lara, D. Serafini, A. Restovic, J.L. Gautier, Synthesis and characterization of manganese–cobalt solid solutions prepared at low temperature, J. Chil. Chem. Soc. 55 (2010) 261–265.
[9] D. Jarosch, Miner. Crystal structure Refinement and Reflectance Measurements of Hausmannite, $Mn_3O_4$, Miner. Petrol 37 (1987) 15–23.
[10] M.B. Salamon, The Physics of manganites: structures and transport, Rev. Mod. Phys. 73 (2001) 583–628.
[11] S.T. Kshirsagar, A.B. Biswas, Crystallographic studies of some mixed manganite spinels, J. Phys. Chem. Solids 28 (1967) 1493–1499.
[12] S. Guillemet-Fritsch, C. Tenailleau, H. Bordeneuve, A. Rousset, Magnetic properties of cobalt and manganese oxide spinels ceramics, Adv. Sci. Technol. 67 (2010) 143–148.
[13] H. Bordeneuve, A. Rousset, C. Tenailleau, S. Guillemet-Fritsch, Cation distribution in manganese cobaltite spinels $Co_{3-x}Mn_xO_4$ ($0 \le x \le 1$) determined by thermal analysis, J. Therm. Anal. Calorim. 101 (2010) 137–142.
[14] X. Chen, P.Y. Hou, C.P. Jacobson, S.J. Visco, L.C.D. Jonghe, Protective coating on stainless steel interconnected for SOFC's: oxidation kinetics and electrical properties, Solid Sate Ionics 176 (2005) 425–433.

[15] H. Bordeneuve, C. Tenailleau, S. Guillemet-Fritsch, R. Smith, E. Suard, A. Rousset, Structural variations and cation distributions in $Mn_{3-x}Co_xO_4$ ($0 \le x \le 3$) dense ceramics using neutron diffraction data, Solid State Sci. 12 (2010) 379–386.

[16] B.L. Ahuja, A. Dashora, N.L Heda, S. Tiwari, N.E Rajeevan, M Itou, Y. Sakurai, R. Kumar, Reversal of orbital magnetic moment on substitution of Bi in multiferroic $Co_2MnO_4$: a magnetic Compton scattering study, Appl. Phys. Lett. 97 (2010) 2125021–2125023.

[17] G.V. Bazuev, A.V. Korolyov, Magnetic behavior of $MnCo_2O_{4+\delta}$ spinel obtained by thermal decomposition of binary oxalates, J. Magn. Magn. Mater. 320 (2008) 2262–2268.

[18] O.I. Gyrdasova, G.V. Bazuev, I.G. Grigorov, O.V. Koryakova, Neorg. Preparation of $MnCo_2O_4$ Whiskers and Spheroids through Thermal Decomposition of $Mn_{1/3}Co_{2/3}C_2O_4 \cdot 2H_2O$, Mater. Res. Bull. 42 (2006) 1234–1241.

[19] F.M.M. Borges, D.M.A. Melo, M.S.A. Câmara, A.E. Martinelli, J.M. Soares, J.H. de Araújo, F.A.O. Cabral, Magnetic behavior of nanocrystalline $MnCo_2O_4$ spinels, J. Magn. Magn. Mater. 302 (2006) 273–277.

[20] P.N. Lisboa-Filho, M. Bahout, P. Barahona, C. Moure, O. Peña, Oxygen stoichiometry effects in spinel-type $NiMn_2O_{4-\delta}$ samples, J. Phys. Chem. Sol. 66 (2005) 1206–1212.

[21] P.N. Lisboa-Filho, A.W. Mombrú, H. Pardo, W.A. Ortiz, E.R. Leite, Influence of processing conditions on the crystal structure and magnetic behavior $La_{0.7}Ca_{0.3}MnO_{3\pm\delta}$ samples, J. Phys. Chem. Sol. 64 (2003) 583–591.

[22] M. Motta, C.V. Deimling, M.J. Saeki, P.N. Lisboa-Filho, Chelating agent effects in the synthesis of mesoscopic-size superconducting particles, J. Sol–Gel Sci. Technol. 46 (2008) 201–207.

[23] N.V. Kosova, N.F. Uvarov, E.T. Devyatkina, E.G. Avvakumov, Mechanochemical synthesis $LiMn_2O_4$ cathode material for lithium batteries, Solid State Ion. 135 (2000) 107–114.

[24] T. Hungría, C. Correas, F. Houdellier, O. Peña, E. Vila, A. Castro, Study of Nanocrystalline $BiMnO_3$–$PbTiO_3$: synthesis, structural elucidation, and magnetic characterization of the whole solid solution, Chem. Eur. J. 18 (2012) 9075–9082.

[25] M.E. Dos-Santos, P.N. Lisboa-Filho, F. Gouttefangeas, O. Peña, Intrinsic magnetic properties of $Bi_xCo_{2-x}MnO_4$ spinels obtained by short-time etching, J. Magn. Magn. Mater. 339 (2013) 157–162.

[26] L.-W. Tai, P.A. Lessing, Modified resin-intermediate processing of perovskite powders: Part II. Processing for fine, nonagglomerated Sr-doped lanthanum chromite powders, J. Mater. Res. 7 (1992) 511–519.

[27] N.E. Rajeevan, R. Kumar, D.K. Sukla, P.P. Pradyumnan, S.K. Arora, I.V. Shvets, Structural, electrical and magnetic properties of Bi-substituted $Co_2MnO_4$, Mater. Sci. Eng. B 163 (2009) 48–56.

[28] A. Petric, H. Ling, Electrical conductivity and thermal expansion of spinels at elevated temperatures, J. Am. Ceram. Soc. 90 (2007) 1515–1520.

[29] M.E. Dos-Santos, R.A. Ferreira, P.N. Lisboa-Filho, O. Peña, Cation distribution and magnetic characterization of the multiferroic cobalt manganese $Co_2MnO_4$ spinel doped with bismuth, J. Magn. Magn. Mater. 329 (2013) 53–58.

[30] P.Y. Mahieux, J.E. Aubert, M. Cyr, M. Coutand, B. Husson, Waste Manage. 30 (2010) 378.

[31] S.G. Antonio, F.R. Benini, F.F Ferreira, P.C.P. Rosa, C.O. Paiva-Santos, Quantitative phase analyses through the Rietveld method with X-ray powder diffraction data of heat-treated carbamazepine Form III, Eur. J. Pharm. Sci. 100 (7) (2011) 2658–2664.

[32] L.G Cançado, K. Takai, T. Enoki, M. Endo, Y.A Kim, H. Mizusaki, A. Jorio, L.N. Coelho, R. Magalhães-Paniago, M.A Pimenta, General equation for the determination of the crystallite size La of nanographite by Raman spectroscopy, Appl. Phys. Lett. 88 (2006) 1631061–1631063.

[33] N.E. Rajeevan, P.P. Pradyumnan, R. Kumar, D.K. Shukla, S. Kumar, A. K. Singh, S. Patnaik, S.K. Arora, I.V. Shvets, Magnetoelectric properties of $Bi_xCo_{2-x}MnO_4$ ($0 < x < 0.3$), Appl. Phys. Let. 92 (2008) 1029101–1029103.

[34] S.K. Sharma, R Kumar, V.V.S Kumar, S.N Dolia, Size dependent magnetic behavior of nanocrystalline spinel ferrite $Mg_{0.95}Mn_{0.05}Fe_2O_4$, Indian J. Pure Appl. Phys. 45 (2007) 16–20.

[35] J. Chen, X. Wu, A. Selloni, Electronic structure and bonding properties of cobalt oxide in the spinel structure, Phys. Rev. B 83 (2011) 2452041–2452047.